

## 18th ESV Paper

### Crash Pulse Modeling for Vehicle Safety Research

Michael S. Varat

Stein E. Husher

KEVA Engineering

United States of America

Paper 501

#### ABSTRACT

Computer simulation, component testing, and sled tests often require the generation of suitable, derived acceleration time histories to define a collision event. These time histories have shape, amplitude, and duration characteristics. Suitable, derived acceleration time histories should be based on a particular vehicle's response in a staged full scale crash test. A staged crash test includes instrumentation in order to measure acceleration time histories, force time histories and other engineering parameters. Analytical techniques are developed to derive acceleration time histories at different collision severities based on the measured acceleration time history in a particular crash test.

#### BACKGROUND

The dependence of occupant response on the collision pulse shape is well studied. Agaram [1] conducted DYNA 3D and MADYMO studies and concluded that "different crush pulses with identical average accelerations values yield different occupant response." The Agaram study [1] used square, triangle and half sine pulse models .

Simulation software has been developed and utilized in the automotive safety field to develop and scale collision pulses. The Structural Impact Simulation and Model Extraction (SISAME) program has been developed under contract with the U.S. Department of Transportation to extract optimal lumped-parameter structural impact models from actual or simulated vehicle crash event data. This program models a vehicle using a lumped parameter methodology. This methodology utilizes rigid masses connected by load paths consisting of zero mass elements. The SISAME program requires a significant modeling effort in order to arrive at scaled collision pulses.

#### INTRODUCTION

This study presents closed form functions that are applied and compared to observed experimental pulse

shapes. Differences between analytical predictions and observed experimental results are explored. Time histories are examined for the same vehicle at different collision test speeds in order to investigate the rate sensitivity of the vehicle collision response. The analytical determination of static crush, dynamic crush and vehicle structural restitution is discussed. This research will show that a vehicle's pulse shape can be modeled and scaled using readily available crash test data fitted with closed form functions.

There are numerous factors that can effect the characteristics of a crash pulse. Some of these include the vehicle shape, vehicle structure, vehicle mass, collision partner, crash mode, and amount of engagement. Given this variability, the modeling technique must be flexible enough to accommodate a wide range of characteristics but robust enough to give good correlation to the parameters modeled.

The presented methodology first examined a set of predefined crash pulse shapes and then interpreted an actual test pulse to develop the parameters that best fit the given shape. The next step was to develop a methodology to scale those characteristics in order to run analytical simulations or tests at different test speeds.

#### PULSE MODELING DERIVATIONS

This research focused on four well recognized and identified shapes: Haversine ( $\sin^2$ ), sine, square wave, and symmetric triangular. The procedure is to use the minimum amount of variables to define the collision pulse. Additionally, the generalized model is derived for a two vehicle collision. The parameters considered are:

a = acceleration

t = time

s = displacement

P = peak acceleration

T = duration of impact

$V_1$  = initial velocity of vehicle 1

$V_2$  = initial velocity of vehicle 2

$\Delta V_1$  = change in velocity of vehicle 1

$\Delta V_2$  = change in velocity of vehicle 2

T = Collision Pulse Time duration

The model inputs:

- $V_{O1}$  = Impact Velocity of Vehicle 1
- $V_{O2}$  = Impact Velocity of Vehicle 2
- $\Delta V_1$  = Velocity Change of Vehicle 1
- $\Delta V_2$  = Velocity Change of Vehicle 2
- Mutual crush = total crush to both Vehicles

Outputs from the model will include the acceleration, velocity, and displacement time histories. Additionally, peak acceleration, average acceleration, and impact duration are also output from the models.

The Haversine pulse, Figure 1, is used as an example of the model development. This pulse has been widely used to represent frontal barrier pulses and has been identified in previous research as being a good representation of a frontal barrier collision pulse [3].

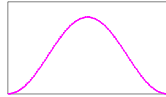


**Figure 1. Haversine pulse.**

The half period sine pulse, Figure 2, is also utilized. This has been previously identified in collision pulse modeling as a standard pulse to represent a frontal barrier impact [3,1].



**Figure 2. Sine pulse.**

The square wave, Figure 3, which represents the collision as a constant acceleration, is presented as the simplest representation of a collision [3,1].

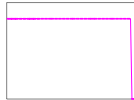


**Figure 3. Square wave pulse.**

The symmetric triangular pulse shape, Figure 4, is modeled. This pulse shape has also been previously identified as a useful collision pulse model [2].



**Figure 4. Triangular pulse.**

The development of the Haversine model is presented here as an example. The sine, triangular, and square wave collision pulse models are derived in the Appendix.

**Model 1: Haversine (Sin<sup>2</sup>).**

The acceleration is written in Equation 1.

$$a = P \sin^2\left(\frac{\pi t}{T}\right) \quad (1).$$

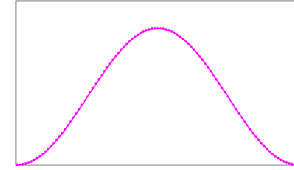


**Figure 12. Graphical representation: Sin<sup>2</sup>.**

Integrating acceleration with respect to time yields velocity.

$$V = \frac{P}{4\pi} \left[ 2\pi t - T \cdot \sin\left(\frac{2\pi t}{T}\right) \right] + C_1 \quad (2).$$

The integration constant  $C_1$  can be evaluated by the initial conditions of  $t = 0$ ,  $V = V_o$  to get  $C_1 = V_o$

Substituting  $C_1$  into Equation 2 yields

$$V = \frac{P}{4\pi} \left[ 2\pi t - T \cdot \sin\left(\frac{2\pi t}{T}\right) \right] + V_o \quad (3).$$

At  $t = T$ ,  $V = V_o + \Delta V$ . Substituting into Equation 3 yields peak acceleration.

$$P = \frac{2 \cdot \Delta V}{T} \quad (4).$$

Integrating Equation 3 yields displacement

$$S = \frac{T^2 \cdot P \cdot \cos\left(\frac{2\pi t}{T}\right) + 2\pi^2 \cdot t(Pt + 4V_o)}{8\pi^2} + C_2 \quad (5).$$

At  $t = 0$ ,  $s = 0$ . Solving for  $C_2$  yields

$$C_2 = \frac{-T^2 \cdot P}{8\pi^2} \quad (6).$$

Substituting  $C_2$  into Equation 5 yields the displacement as a function of time

$$S = \frac{T^2 \cdot P}{8\pi^2} \left[ \cos\left(\frac{2\pi t}{T}\right) - 1 \right] + \frac{t}{4} (Pt + 4V_o) \quad (7).$$

The final parameter to be determined is the duration of contact. At  $t_1 = t_2 = T$ , mutual crush = absolute value of  $s_1 - s_2$ . Solving Equation 7 for impact duration results in the following determination of duration.

$$T = \frac{\text{mutual crush}}{\text{abs} \left[ \frac{1}{2} (\Delta V_1 - \Delta V_2) + (V_{o_1} - V_{o_2}) \right]} \quad (8).$$

The development of the above pulse shape (and those in the appendix) cover a wide range of characteristic shapes to approximate a crash pulse. However, the demonstrated methodology can be applied to most integrable functions which allows the user to customize this methodology to other pulse shapes.

### MODEL APPLICATIONS

After the pulse shape has been selected and the various characteristics of the function have been derived, there are a number of factors that arise in the application of the derived model. When fitting a model to actual crash test data it is simple to determine the  $\Delta V$  from the instrumentation; however, the crush is not as easily quantified and various difficulties arise as to exactly what crush value to use.

A careful review of the derivation of the model reveals that the use of the crush at separation of the collision partners is required. The crush at separation is easily determined from a derived force deflection chart as seen in Figure 5. This separation crush was input into the model for the sample test and the four models were developed. Shown in Figure 6 are the resulting four models plotted with the actual acceleration time history. The data is then integrated and the resulting velocity time histories are shown in Figure 7. This is integrated again and the resulting displacement time histories are shown in Figure 8.

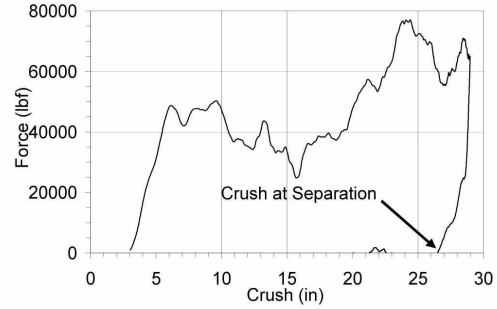


**Figure 5. Force versus deflection – compact four door sedan.**

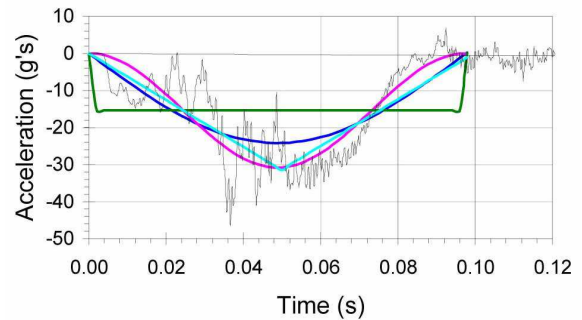


**Figure 6. Crush at separation as input into the pulse models – acceleration versus time.**

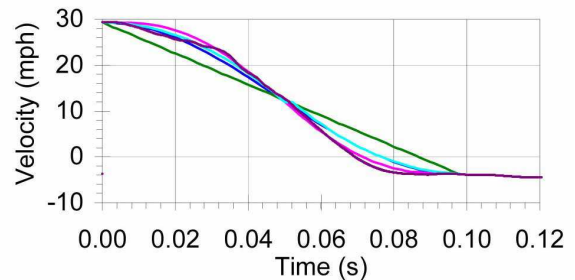


**Figure 7. Crush at separation as input into the pulse models – velocity versus time.**

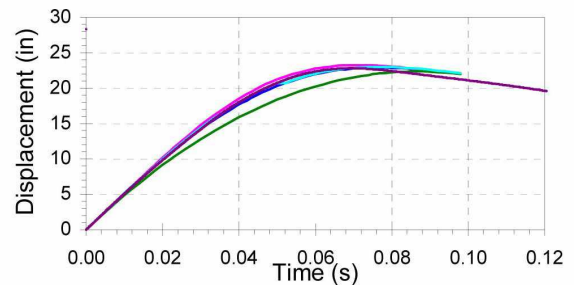


**Figure 8. Crush at separation as input into the pulse models – displacement versus time.**

## STRUCTURAL RESPONSE

Analysis of the acceleration and force data generated provides some insight into the structural response characteristics of the vehicle. For this analysis restitution and crush rate sensitivity are considered. Depicted in Figure 9 is an absorbed energy parameter [4] for the frontal barrier tests conducted on a front engine, front wheel drive midsize hatchback at 56, 64 and 77 kph. This graph indicates that there is good correlation with energy absorption as velocity increases.

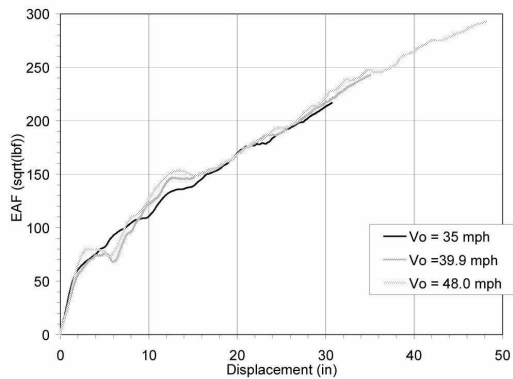


**Figure 9. Comparison of EAF versus deflection derived from a front engine front wheel drive midsize hatchback tested at different velocities.**

Figure 10 is an energy absorption graph of a small pickup truck undergoing frontal barrier impacts at 24 and 56 kph. There is similar structural response of these 2 tests except in the very elastic initial 100 mm of deformation. It is apparent that the energy absorption characteristics follow the same path; that is similar amounts of deformation require similar amounts of energy irrespective of test speed.

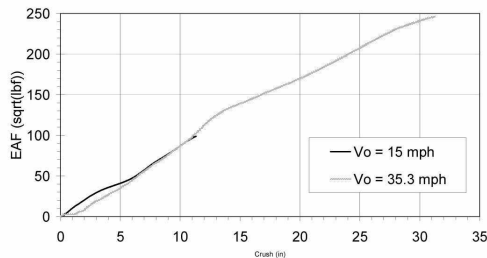


**Figure 10. Comparison of EAF versus deflection derived from tests at different velocities – small pickup truck.**

## RESTITUTION CHARACTERISTICS

After the maximum mutual crush has occurred the impacting vehicle structures begin to rebound. The

restitution characteristics have a significant influence on the post impact structural deformation data when considering what is occurring in the dynamic environment. The force deflection of a mid size four door sedan full scale barrier test is plotted and shown in Figure 11. The figure shows the maximum dynamic structural deformation is about 750 mm. At the moment of separation from the barrier the deflection of the vehicle is about 675 mm. The measured static residual crush is about 490 mm. This difference between crush at separation and residual crush has been observed in numerous other frontal barrier tests and indicates that vehicle structures continue to restore after separation from the barrier has occurred. The rate of restoration is not sufficient to maintain contact with the load cell barrier face.

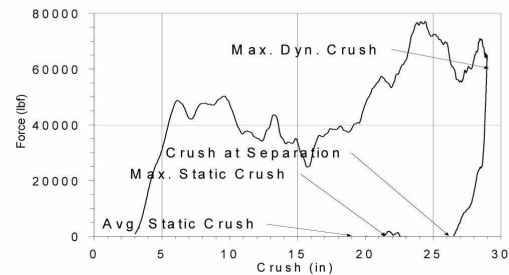


**Figure 11. Force versus deflection – midsize four door sedan.**

## VELOCITY SENSITIVITY

An investigation was performed to analyze whether a particular vehicle is well modeled by a characteristic shape at different test speeds. If a vehicle can be represented by a characteristic shape, then that shape can be determined from a compliance test and readily scaled to a different speed. While this concept has not been generalized it has been observed in numerous tests that have been analyzed. Two of those studies are presented for discussion here.

Acceleration data from two rigid frontal barrier crash tests of the same model full size van were studied and shown in Figures 12 and 14. Overlaid on these acceleration time histories is a sine model using the presented methodology. Examination of the resulting velocity time histories (Figures 13 and 15) demonstrates clearly that the sine model represents the vehicle dynamics. Even though these tests differ by a factor of 4 in energy, the characteristic pulse shape is the same

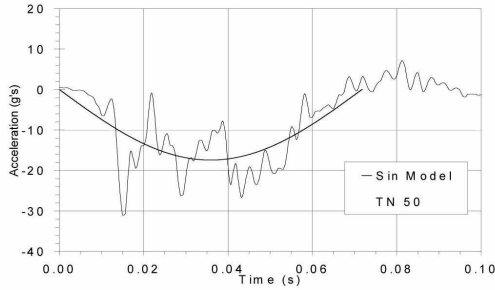


**Figure 12. Acceleration versus time for a full size van at 25 kph. Sine fit.**

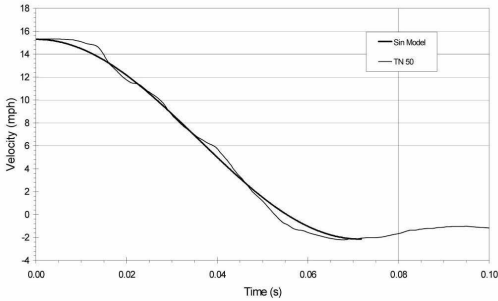


**Figure 13. Velocity Versus Time for a full size van at 25 kph. Sine fit.**

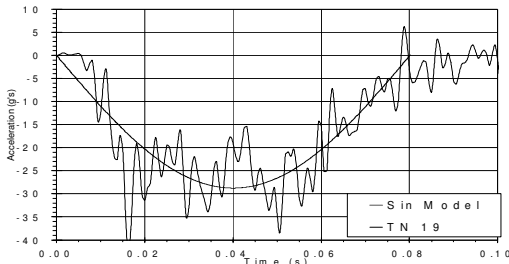


**Figure 14. Acceleration versus time for a full size van at 48 kph. Sine fit.**

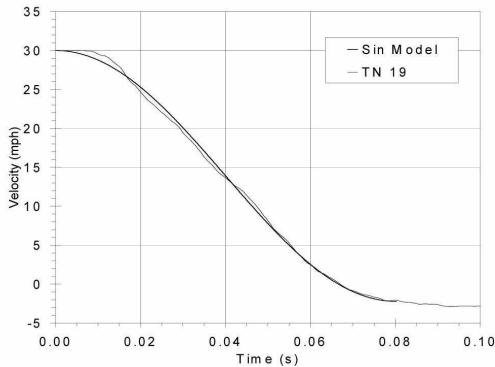


**Figure 15. Velocity versus time for a full size van at 48 kph. Sine fit.**

A second analysis is performed with frontal barrier crash tests of a small four door sedan at 40, 48 and 57 kph - Figures 16-18. The sine model, again, best represents this vehicle's collision time history at all three test speeds. In the course of this research, other vehicles were studied with similar results. These results indicate that determined characteristic shape can be scaled to different speeds for similar impact conditions.

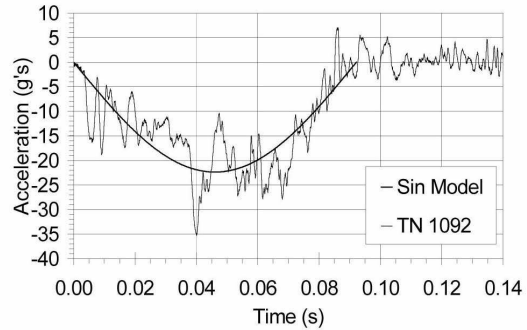


**Figure 16. Acceleration versus time for small four door sedan at 40 kph. Sine fit.**

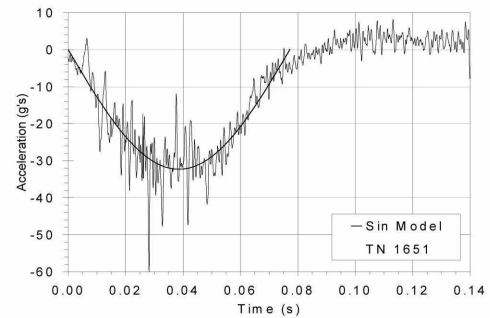


**Figure 17. Acceleration versus time for small four door sedan at 48 kph. Sine fit.**

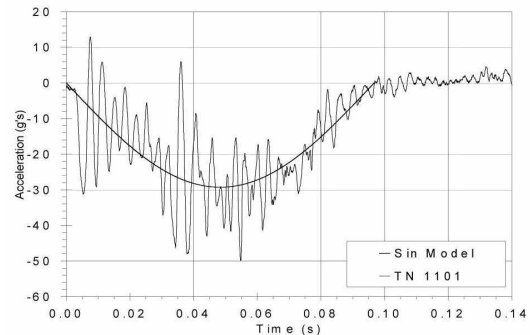


**Figure 18. Acceleration versus time for small four door sedan at 57 kph. Sine fit.**

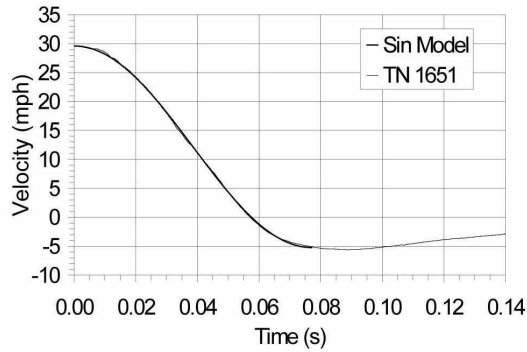


**Figure 19. Velocity versus time for small four door sedan at 40 kph. Sine fit.**

### MODELING DIFFERENT COLLISION MODES

The generated crash pulses have been compared to full engagement barrier testing. In order to study the effect of impact configuration, a comparison was made between a full engagement barrier test and an offset deformable barrier test. Figures 20 and 21 show the sine fit to the full engagement test acceleration data.

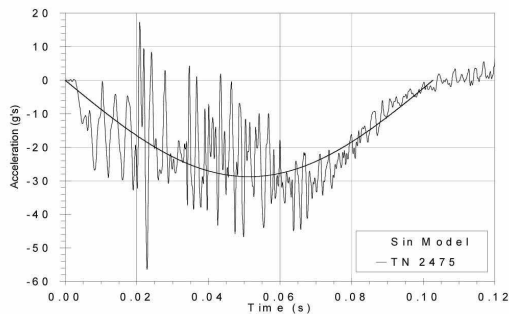


**Figure 20. Acceleration versus time for a mid size four door sedan full frontal impact at 56 kph. Sine fit.**

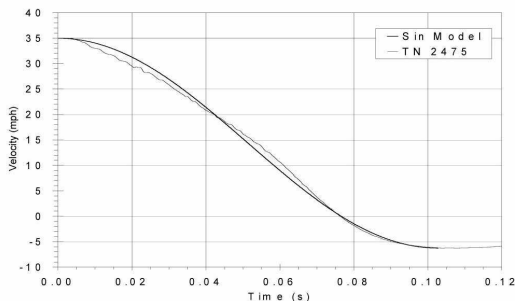


**Figure 21. Velocity versus time for a mid size four door sedan full frontal impact at 56 kph. Sine fit.**

Utilizing the same modeling technique, it was determined that for the offset test a triangular pulse was a better model. The triangular pulse is fitted to

the acceleration and the velocity time histories as shown in Figures 22 and 23. The full engagement test is best represented by the sine model. In contrast the offset deformable test is best represented by the triangular model. Consequently, impact mode clearly effects the pulse shape. Additional work must be done in order to generalize a method that will account for the differences observed in two different crash modes.

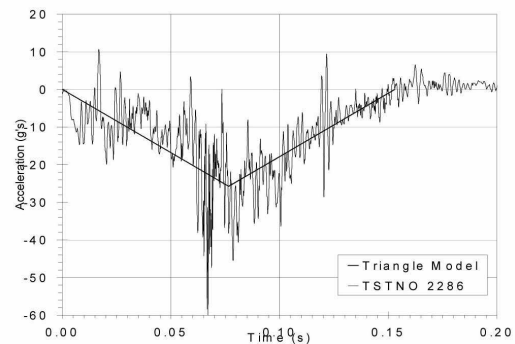


**Figure 22. Acceleration versus time for a mid size four door sedan 40% offset impact at 64 kph. Triangular fit.**

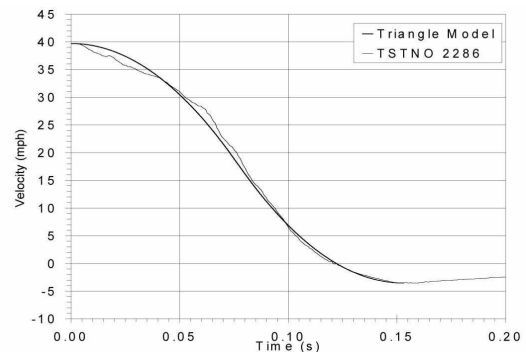


**Figure 23. Velocity versus time for a mid size four door sedan 40% offset impact at 64 kph. Triangular fit.**

### CONCLUSIONS

- The derived collision pulse models have been shown to represent the response of a vehicle undergoing an impact.
- The applied technique is easily expandable to other geometric pulse shapes.
- The derived models have been shown to be scalable to other impact severities, but care must be exercised in the application

- Structural response of the vehicle is dependant on many characteristics which include vehicle and impact mode parameters.
- Different crash modes with the same vehicle can exhibit different collision pulse shapes.
- Inputs to the collision pulse models must be carefully considered. Impact speed,  $\Delta V$ , and crush data require careful analysis.
- For the vehicles studied, some vehicle structural rebound takes place after separation from the barrier. This phenomenon prevents the structural rebound from being directly measured by either load cell or accelerometer instrumentation.
- Care must be exercised when applying the data in this present research to a specific vehicle.

## CONTACT

Questions and comments are welcome and should be addressed to the authors at:

KEVA Engineering, LLC  
601 Daily Dr. Suite 225  
Camarillo, California 93010  
[www.kevaeng.com](http://www.kevaeng.com)

## REFERENCES

- [1] Agaram, V., Xu, L., Wu, J., Kostyniuk, G., Nusholtz, G. Comparison of Frontal Crashes in Terms of Average Acceleration, SAE Technical Paper 2000-01-0880, Society of Automotive Engineers, Warrendale, PA, 2000.
- [2] Brach, R.M., Mechanical Impact Dynamics, John Wiley and Sons, Inc., New York, NY, 1991.
- [3] Breed, D.S., Castelli, V., Sanders, W.T., A New Automobile Crash Sensor Tester, SAE Technical Paper 910655, Society of Automotive Engineers, Warrendale, PA, 1991.
- [4] Kerkhoff, J.F., Husher, S.E., Varat, M.S., Busenga, A.M., Hamilton, K., An Investigation into Vehicle Frontal Impact Stiffness, BEV, and Repeated Testing for Reconstruction, SAE Technical Paper 930899, Society of Automotive Engineers, Warrendale, PA, 1993.

[5] Varat, M., Husher S., Vehicle Impact Response Analysis Through the Use Of Accelerometer Data, , SAE Technical Paper 2000-01-0850, Society of Automotive Engineers, Warrendale, PA, 2000

[6] Wooley R. L., Non-Linear Damage Analysis in Accident Reconstruction, SAE Technical Paper 2001-01-0504, Society of Automotive Engineers, Warrendale, PA, 2001

## APPENDIX – Sinusoidal, Square, and Triangular Pulse Derivations

### Model 2: Sinusoidal Pulse.

The model evaluated is a sine model to represent the acceleration pulse.

$$a = P \sin(\theta) \quad (2-1).$$

$$\theta = \frac{\pi t}{T} \quad (2-2).$$

where theta is chosen with boundary conditions that at  $t = 0$ ,  $a = 0$  and at  $t = T$ ,  $a = 0$ .

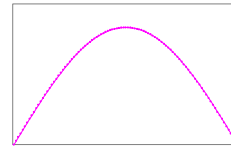


**Figure A. Graphical Representation: Sine.**

Integrating this acceleration yields the relationship for the velocity.

$$V = \frac{-T \cdot P \cdot \cos\left(\frac{\pi t}{T}\right)}{\pi} + C_1 \quad (2-3).$$

The integration constant  $C_1$  can be evaluated using the initial condition: at  $t = 0$ ,  $V = V_0$ .

$$C_1 = \frac{T \cdot P}{\pi} + V_0 \quad (2-4).$$

Substituting  $C_1$  into Equation 2-3

$$V = \frac{-T \cdot P \cdot \cos\left(\frac{\pi t}{T}\right)}{\pi} + \frac{T \cdot P}{\pi} + V_0 \quad (2-5).$$

The peak acceleration (P) can be found by solving Equation 2-5 knowing that at  $t = T$ ,  $V = V_0 + \Delta V$ .

$$P = \frac{\Delta V \cdot \pi}{2 \cdot T} \quad (2-6).$$

The integration of velocity yields displacement.

$$S = \frac{-T^2 \cdot P \cdot \sin\left(\frac{\pi t}{T}\right)}{\pi^2} + t \left( V + \frac{T \cdot P}{\pi} \right) + C_2 \quad (2-7).$$

$C_2$  is solved by knowing that at  $t = 0$ ,  $s = 0$ , therefore

$$C_2 = 0 \quad (2-8).$$

Substituting  $C_2$  into Equation 2-7 gives displacement

$$S = \frac{-T^2 \cdot P \cdot \sin\left(\frac{\pi t}{T}\right)}{\pi^2} + t \left( V + \frac{T \cdot P}{\pi} \right) \quad (2-9).$$

The acceleration, velocity, and displacement time histories all require the collision duration. The collision duration is determined through the following additional boundary condition: at  $t_1 = t_2 = T$ , mutual crush =  $s_1 - s_2$ . Substituting these conditions into the displacement time equation, yields the following equation for duration,  $T$ .

$$T = \frac{\text{mutual crush}}{\text{abs} \left[ (V_{o_1} - V_{o_2}) + \left( \frac{\Delta V_1}{2} - \frac{\Delta V_2}{2} \right) \right]} \quad (2-10).$$

### **Model 3: Square Pulse.**

The third derived model is that of a simple square wave. For this relationship, peak and average accelerations are equal throughout the entire collision duration.

$$a = P \quad 0 \leq t \leq T \quad (3-1).$$

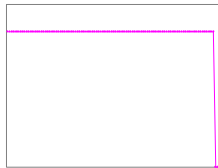


**Figure B. Graphical Representation: Square.**

The integration of acceleration with respect to time yields velocity

$$V = Pt + C_1 \quad (3-2).$$

At  $t=0$ ,  $V = V_o$ . Solving for  $C_1$

$$C_1 = V_o \quad (3-3).$$

Substituting  $C_1$  into Equation 3-2

$$V = Pt + V_o \quad (3-4).$$

Solving for  $P$  at  $t = T$ ,  $V = V_o + \Delta V$ . The peak acceleration can now be determined. Note that the peak acceleration equals the average acceleration in this model.

$$P = \frac{\Delta V}{T} \quad (3-5).$$

Integrate velocity to get displacement

$$S = \frac{1}{2} Pt^2 + V_o t + C_2 \quad (3-6).$$

At  $t = 0$ ,  $S = 0$ .  $C_2$  can now be determined.

$$C_2 = 0 \quad (3-7).$$

Substituting  $C_2$  into Equation 3-6

$$S = \frac{1}{2} Pt^2 + V_o t \quad (3-8).$$

At  $t_1 = t_2 = T$ , mutual crush = absolute value of  $S_1 - S_2$ . Solving for duration yields

$$T = \frac{\text{mutual crush}}{\text{abs} \left[ \frac{1}{2} (\Delta V_1 - \Delta V_2) + (V_{o_1} - V_{o_2}) \right]} \quad (3-9).$$

### **Model 4: Triangular Pulse**

The final derived model is that of a triangular wave.

$$\left[ \begin{array}{l} a = \frac{2P}{T} \cdot t \quad 0 \leq t \leq \frac{T}{2} \\ a = \frac{-2P}{T} \cdot t + 2P \quad \frac{1}{2}T < t \leq T \end{array} \right] \quad (4-1).$$





**Figure C. Graph. Representation: Triangular.**

The analysis of the triangular pulse is going to be performed in two parts. First, the time up to  $t \leq \frac{1}{2} T$  is analyzed. For this time period, velocity is found by the integration of Equation 20 with respect to time.

$$V = \frac{P}{T} \cdot t^2 + C_1 \quad (4-2).$$

Using the known conditions,  $V = V_o$  at  $t = 0$ ,  $C_1$  can be determined

$$C_1 = V_o \quad (4-3).$$

Substituting  $C_1$  into Equation 4-3

$$V = \frac{P}{T} t^2 + V_o \quad \text{For } t \leq \frac{1}{2} T \quad (4-4).$$

Since the assigned triangular acceleration pulse is symmetrical about the midpoint, at time  $t = \frac{1}{2} T$ , the change in velocity will equal one half of the total change in velocity.

$$\text{At } t = \frac{T}{2} \quad V = \text{abs}(V_o - \frac{1}{2} \Delta V) \quad (4-5).$$

Assigning these boundary conditions allows the solution for the peak acceleration

$$P = \frac{2\Delta V}{T} \quad (4-6).$$

Integrating Equation 4-4 with respect to time yields displacement

$$S = \frac{P}{3 \cdot T} t^3 + V_o t + C_2 \quad (4-7).$$

At  $t = 0$ ,  $s = 0$ . This allows the determination of  $C_2$ .

$$C_2 = 0 \quad (4-8)$$

Substituting  $C_2$  into Equation 4-7

$$S = \frac{P}{3 \cdot T} t^3 + V_o t \quad \text{For } t \leq \frac{1}{2} T \quad (4-9).$$

The preceding derivation must now be carried out for

$$t \geq \frac{1}{2} T \quad (4-10).$$

Velocity is found by integrating Equation 4-9 with respect to time

$$V = \frac{-P}{T} t^2 + 2Pt + C_1 \quad (4-11).$$

$C_1$  is arrived at by solving Equation 4-11 at time equal to one half of the duration.

$$V = \frac{P \cdot T}{4} + V_o \quad (4-12)$$

Setting Equation 4-11 equal to Equation 4-12 allows for  $C_1$  to be solved for.

$$C_1 = V_o - \frac{1}{2} P \cdot T \quad (4-13)$$

Substituting  $C_1$  into Equation 4-11 gives velocity

$$V = \frac{-P}{T} t^2 + 2Pt + V_o - \frac{1}{2} P \cdot T \quad \text{For } t \geq \frac{1}{2} T \quad (4-14).$$

Integration of Equation 4-14 yields displacement

$$S = \frac{-P}{3T} t^3 + Pt^2 + V_o t - \frac{1}{2} P \cdot T \cdot t + C_2 \quad (4-15).$$

By setting Equation 4-9 equal to Equation 4-15 at time equal to half the duration,  $C_2$  can be determined.

$$C_2 = \frac{PT^2}{12} \quad (4-16).$$

Substituting  $C_2$  into Equation 4-15 results in:

$$S = \frac{-P}{3T} t^3 + Pt^2 + V_o t - \frac{1}{2} P \cdot T \cdot t + \frac{PT^2}{12} \quad \text{For } t \geq \frac{1}{2} T \quad (4-17).$$

Combining the two derived relationships for displacements up to the collision mid point and then after the collision midpoint, the duration can be determined. At time  $t = T$ , the mutual crush = absolute value of  $s_1 - s_2$ . Algebraically solving for duration of impact yields the following:

$$T = \frac{\text{mutual crush}}{\text{abs}\left[\frac{2}{3}(\Delta V_1 - \Delta V_2) + (V_{o_1} - V_{o_2})\right]} \quad (4-19).$$